

## High-pressure Raman study of $\text{Al}_2(\text{WO}_4)_3$

M. Maczka,<sup>a,\*</sup> W. Paraguassu,<sup>b</sup> A.G. Souza Filho,<sup>b</sup> P.T.C. Freire,<sup>b</sup> J. Mendes Filho,<sup>b</sup>  
F.E.A. Melo,<sup>b</sup> and J. Hanuza<sup>a,c</sup>

<sup>a</sup>Institute for Low Temperature and Structure Research, Polish Academy of Sciences, P.O. Box 1410, 50-950 Wrocław 2, Poland

<sup>b</sup>Departamento de Física, Universidade Federal do Ceará, P.O. Box 6030, Fortaleza-CE 60455-900, Brazil

<sup>c</sup>Faculty of Industry and Economics, University of Economics, 118/120 Komandorska Str., 53-345 Wrocław, Poland

Received 21 October 2003; received in revised form 19 December 2003; accepted 23 January 2004

### Abstract

A high-pressure Raman scattering study of the tungstate  $\text{Al}_2(\text{WO}_4)_3$  is presented. This study showed the onset of two reversible phase transitions at  $0.28 \pm 0.07$  and  $2.8 \pm 0.1$  GPa. The pressure evolution of Raman bands provides strong evidences that both the transitions involve rotations/tilts of nearly rigid tungstate tetrahedra and that the structure of the stable phase in the 0.28–2.8 GPa range may be the same as the structure of the ambient pressure, low-temperature monoclinic ( $C_{2h}^5$ ) ferroelastic phase of  $\text{Al}_2(\text{WO}_4)_3$ . © 2004 Elsevier Inc. All rights reserved.

**Keywords:** High pressure; Phase transition; Raman spectra

### 1. Introduction

$\text{Al}_2(\text{WO}_4)_3$  belongs to the  $A_2(\text{BO}_4)_3$  group of compounds ( $A = \text{Cr}, \text{Al}, \text{Sc}, \text{In}$ ;  $B = \text{Mo}, \text{W}$ ) that have been the subject of considerable interest in recent years due to their interesting physical and chemical properties. Firstly, these compounds exhibit a temperature-induced ferroelastic phase transition from an orthorhombic ( $D_{2h}^{14} = Pnca$ ) to a monoclinic ( $C_{2h}^5 = P2_1/a$ ) structure [1–3]. Secondly, the orthorhombic phase of  $A_2(\text{MoO}_4)_3$  molybdates, where  $A = \text{Fe}, \text{Cr}, \text{Al}, \text{Sc}$ , as well as  $\text{Sc}_2(\text{WO}_4)_3$  tungstate exhibits negative thermal expansion (NTE) [2–6]. The behavior of  $\text{Al}_2(\text{WO}_4)_3$  is less clear: an NTE from dilatometric measurements [4] and a positive thermal expansion from diffraction data [4] have been reported. Thirdly, unusually high trivalent ion conduction has been demonstrated in these crystals [7–10]. Fourthly, a pressure-induced amorphization was discovered recently in  $\text{Sc}_2(\text{MoO}_4)_3$  and  $\text{Sc}_2(\text{WO}_4)_3$  at moderate pressures [10–12]. Fifthly, the  $A_2(\text{BO}_4)_3$  crystals are suitable hosts for transition metal and lanthanide ions. All these features make these crystals suitable for a wide variety of applications in fuel cell

electrolytes [13], gas sensors [13], laser materials [14], electronics [6], catalysts support [6], among others.

Temperature dependence of infrared-active modes of  $\text{Al}_2(\text{WO}_4)_3$  has been previously studied [14]. Recently, some reports have discussed the effects of high pressure on  $\text{Al}_2(\text{WO}_4)_3$  properties [13,15]. The pressure dependence of X-ray diffraction pattern at 400°C was discussed in Ref. [13]. These results suggested the onset of an orthorhombic to tetragonal phase transition at about 3.0 GPa. In Ref. [15] the high-pressure resistivity and compressibility measurements, performed at room temperature, indicated the onset of a reversible phase transition in  $\text{Al}_2(\text{WO}_4)_3$  at about 0.5 GPa.

In the present paper, we report high-pressure Raman studies on  $\text{Al}_2(\text{WO}_4)_3$  in order to get more insight in the nature of the transition reported in Ref. [15]. We observed two reversible phase transitions at  $0.28 \pm 0.07$  and  $2.8 \pm 0.1$  GPa. The present study gives strong indication that the phase, stable between 0.28 and 2.8 GPa, may have the same structure as the ferroelastic monoclinic phase observed at low temperatures. The analysis of the pressure dependence of the various Raman modes suggests that both transitions have as driven mechanism the rotations and/or tilts of the nearly rigid  $\text{WO}_4^{2-}$  tetrahedra.

\*Corresponding author. Fax: +48713441029.

E-mail address: [maczka@int.pan.wroc.pl](mailto:maczka@int.pan.wroc.pl) (M. Maczka).

## 2. Experimental

Single crystals of  $\text{Al}_2(\text{WO}_4)_3$  were grown by cooling of the molten mixture containing  $\text{Al}_2(\text{WO}_4)_3$  and solvent  $\text{Na}_2\text{W}_2\text{O}_7$  in 1:1 ratio. The cooling rate was  $2^\circ\text{C}/\text{h}$  from  $1000^\circ\text{C}$  to  $800^\circ\text{C}$  and  $5^\circ\text{C}/\text{h}$  down to room temperature. The pressure-dependent Raman spectra were obtained with a triple-grating spectrometer (Jobin Yvon T64000) equipped with a  $\text{N}_2$ -cooled charge coupled device detection system. The line 514.5 nm of an argon ion laser was used as excitation. An Olympus microscope lens with a focal distance  $f = 20.5\text{ mm}$  and numeric aperture  $\text{NA} = 0.35$  was used to focus the laser beam on the sample surface. High-pressure Raman experiments were performed using a diamond anvil cell (DAC) with 4:1 methanol:ethanol mixture as transmitting fluid. The pressure calibration was achieved by using the well-known pressure shift of the ruby luminescent lines. The spectrometer slits were set for a resolution of  $2\text{ cm}^{-1}$ . In order to avoid any polarization effect to be observed in the spectra due to eventual rotation of the sample inside the cell during pressure loading, we have used a depolarizer to destroy the polarization of both incident and scattered light beams. The same depolarizer was used to record the spectrum outside the DAC.

## 3. Results and discussion

At room temperature and ambient pressure, the  $\text{Al}_2(\text{WO}_4)_3$  crystallizes in an orthorhombic structure (space group  $D_{2h}^{14} = Pnca$ ,  $Z = 4$ ) with 68 atoms per unit cell [14]. This structure contains a network of corner-sharing  $\text{AlO}_6$  octahedra and  $\text{WO}_4^{2-}$  tetrahedra.  $\text{Al}^{3+}$  ions occupy sites of  $C_1$  symmetry and the  $\text{WO}_4^{2-}$  tetrahedra form two crystallographically distinct sets of  $C_1$  and  $C_2$  symmetry. The factor group analysis leads to 204 degrees of freedom ( $k = 0$ ) distributed among the irreducible representations as  $25A_g + 26B_{1g} + 25B_{2g} + 26B_{3g} + 25A_u + 26B_{1u} + 25B_{2u} + 26B_{3u}$ . Selection rules stand that only  $A_g$ ,  $B_{1g}$ ,  $B_{2g}$  and  $B_{3g}$  modes are Raman active. The 102 Raman-active modes can be subdivided into  $6A_g + 6B_{1g} + 6B_{2g} + 6B_{3g}$  stretching modes,  $8A_g + 7B_{1g} + 8B_{2g} + 7B_{3g}$  bending modes,  $4A_g + 5B_{1g} + 4B_{2g} + 5B_{3g}$  librational modes,  $4A_g + 5B_{1g} + 4B_{2g} + 5B_{3g}$  translational modes of  $\text{WO}_4^{2-}$  tetrahedra, and  $3A_g + 3B_{1g} + 3B_{2g} + 3B_{3g}$  translational modes of the  $\text{Al}^{3+}$  ions (the details can be found in Ref. [14]). The unpolarized Raman spectrum at room temperature and ambient pressure is shown in Fig. 1 (lower trace). A total number of 21 modes could be identified. Although group theory predicts a much larger number of modes, significantly smaller number of modes are observed because in the unpolarized spectrum factor group splitting for majority of modes is not resolved. Based on polarized Raman scattering studies (not discussed in

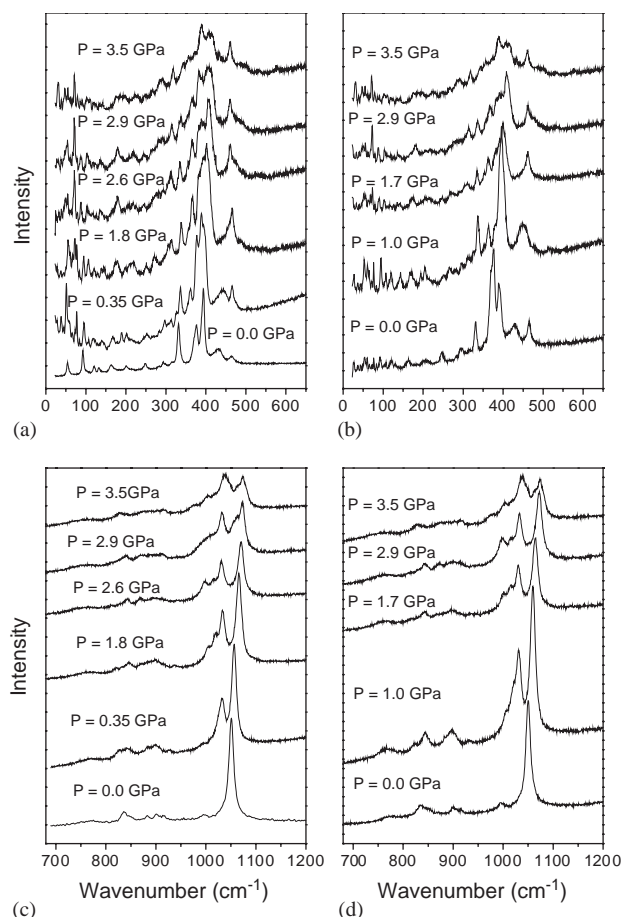


Fig. 1. Raman spectra of  $\text{Al}_2(\text{WO}_4)_3$  crystals recorded at different pressures during compression (a,c) and decompression (b,d) experiments in the (a,b) low- and (c,d) high-wavenumber range.

this paper) [14] and studies on isomorphous material [12], we may easily identify the symmetric stretching modes ( $1030\text{--}1050\text{ cm}^{-1}$ ) and asymmetric stretching modes ( $830\text{--}1000\text{ cm}^{-1}$ ). In a similar way, we may locate the bending modes of the  $\text{WO}_4^{2-}$  tetrahedra in the  $300\text{--}470\text{ cm}^{-1}$ . However, our studies of  $\text{KAl}(\text{MoO}_4)_2$  and  $\text{NaAl}(\text{MoO}_4)_2$  showed that translational motions of  $\text{Al}^{3+}$  ions should be observed in the same wavenumber region as the bending modes [16]. We may expect, therefore, to observe a strong coupling between the same symmetry bending modes and translational modes of the  $\text{Al}^{3+}$  ions. The remaining modes, observed below  $300\text{ cm}^{-1}$ , can be assigned to translational and librational motions of the  $\text{WO}_4^{2-}$  tetrahedra.

On applying pressure, the Raman spectra exhibit significant changes at about  $0.28\text{ GPa}$  (see Fig. 1(a) and 1(c)). A rise of a background can also be noted, especially at  $0.35\text{ GPa}$ . The origin of the background change during the measurements is not clear. However, it does not introduce drawbacks in the analysis. The most characteristic changes are the appearance of new bands at around  $1031$ ,  $360$  and  $38\text{ cm}^{-1}$ , splitting

of 370–400 and 200  $\text{cm}^{-1}$  bands as well as significant wavenumber change for a number of vibrational modes. These changes can be followed in detail by analyzing the wavenumber vs. pressure plot shown in Fig. 2. The results shown in Fig. 2 indicate that the material experiences a discontinuous structural transformation at about 0.28 GPa. The increase in the number of modes, especially in the lattice modes region (see Fig. 2c and Table 1), clearly indicates that the transition leads to a symmetry lowering. However, the overall contour of the stretching bands is similar both at ambient and 0.35 GPa pressure thus indicating that as a result of the pressure-induced transition the W–O bond lengths and O–W–O tetrahedral angles change slightly. The comparison of the spectrum measured at 0.35 GPa with the spectrum of the ferroelastic monoclinic phase of  $\text{Al}_2(\text{WO}_4)_3$  measured at ambient pressure and low

temperature (150 K), shows a remarkable similarity between these spectra as shown in Fig. 3. In particular, the distinctive spectral features of the ferroelastic monoclinic phase are the appearance of new bands around 1032, 359 and 35  $\text{cm}^{-1}$  as well as splitting of the 370–400  $\text{cm}^{-1}$  bands. These results give strong indication that the phase transition at  $0.28 \pm 0.07$  GPa occurs from the  $D_{2h}^{14}$  orthorhombic structure to the  $C_{2h}^5$  monoclinic ferroelastic structure, i.e., the increase of pressure at room temperature seems to induce the same structural changes as temperature lowering at ambient pressure. This transition is known to be a result of  $\text{WO}_4^{2-}$  tetrahedra tilting and is accompanied by 1.33% change in density [14]. It is worth noting that the presence of a reversible phase transition in  $\text{Al}_2(\text{WO}_4)_3$  has recently been reported by resistivity and compressibility studies [15]. These studies indicated the onset of a phase transition at about 0.5 GPa [15]. Moreover, it has been shown that the density of the parent phase increased by 1.4% at the phase transition. As one can note, this density increase is nearly the same as that observed at the temperature-induced orthorhombic to monoclinic phase transition. This result supports, therefore, our conclusion that the phase above 0.28 GPa may be monoclinic and ferroelastic.

By further increasing pressure, the Raman modes show continuous wavenumber and intensity changes. All the peaks observed in the spectra can be well fit with a linear pressure dependence  $\omega(P) = \omega_0 + \alpha P$ . It is worth noting that some of the modes exhibit negative  $\alpha$  values (see Table 1) that are typically observed in materials exhibiting the NTE phenomenon [17,18]. Around  $2.8 \pm 0.1$  GPa significant changes occur in the  $\text{Al}_2(\text{WO}_4)_3$  crystal, i.e., a number of new modes appear, many bands broaden significantly and discontinuities in the slopes of many of the Raman modes are observed. These changes indicate emergence of a new phase at about  $2.8 \pm 0.1$  GPa. However, the observed changes are weak indicating that as a result of this transition the crystal structure changes slightly. In particular, we could not observe the appearance of new modes below 800  $\text{cm}^{-1}$  indicative for significant change in the strength of interactions between the  $\text{WO}_4^{2-}$  tetrahedra at this transition, as observed in the isomorphous compound  $\text{Sc}_2(\text{MoO}_4)_3$  around 2.7 GPa [12]. This result clearly shows that although both  $\text{Sc}_2(\text{MoO}_4)_3$  and  $\text{Al}_2(\text{WO}_4)_3$  seem to exhibit the orthorhombic to monoclinic phase transition below 0.5 GPa, the 2.8 GPa phase transition in  $\text{Al}_2(\text{WO}_4)_3$  results in much weaker structural changes than the 2.7 GPa transition in  $\text{Sc}_2(\text{MoO}_4)_3$ . This difference can be most likely attributed to the fact that the  $\text{Al}_2(\text{WO}_4)_3$  structure is less flexible, when compared to the  $\text{Sc}_2(\text{MoO}_4)_3$  structure, since due to significantly shorter Al–O distances and more covalent Al–O bonds, the  $\text{WO}_4$  tetrahedra are more tightly bounded to the  $\text{AlO}_6$  octahedra than the  $\text{MoO}_4$  tetrahedra to the  $\text{ScO}_6$

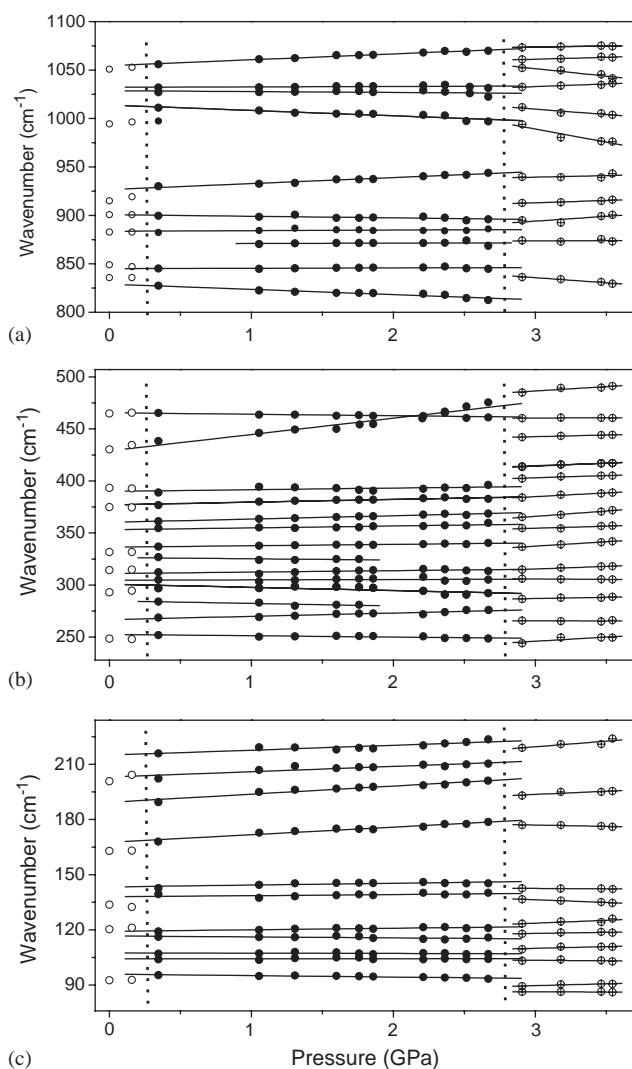


Fig. 2. Wavenumber vs. pressure plot of the (a) high-, (b) medium- and (c) low-wavenumber modes observed in  $\text{Al}_2(\text{WO}_4)_3$  crystals for compression experiments. The solid lines are linear fits on the data to  $\omega(P) = \omega_0 + \alpha P$ .

Table 1

Raman wavenumbers (in  $\text{cm}^{-1}$ ) for the three different phases along with pressure coefficients  $\alpha$  (in  $\text{cm}^{-1} \text{GPa}^{-1}$ ) for the intermediate and high-pressure phases of  $\text{Al}_2(\text{WO}_4)_3$

Ambient pressure phase	Intermediate phase		High-pressure phase		Assignment
	$\omega_0$ ( $\text{cm}^{-1}$ )	$\alpha$ ( $\text{cm}^{-1} \text{GPa}^{-1}$ )	$\omega_0$ ( $\text{cm}^{-1}$ )	$\alpha$ ( $\text{cm}^{-1} \text{GPa}^{-1}$ )	
1051	1056	6.0	1073	2.3	$\text{WO}_4^{2-}$ stretching modes
994	1032	0.5	1061	4.0	
915	1027	-0.5	1052	-15.5	
900	1011	-5.4	1032	5.4	
882	997	-7.9	1012	-11.1	
849	930	5.3	994	-27.0	
836	899	-1.7	940	3.3	
	882	0.9	913	4.8	
	870	0.3	895	9.9	
	845	0.3	874	0.6	
	827	-5.3	836	-10.4	
465	465	-1.4	485	8.5	$\text{WO}_4^{2-}$ bending modes coupled to $\text{Al}^{3+}$ translations
430	428	15.4	460	0.2	
393	389	1.6	442	3.3	
375	377	2.6	414	5.7	
332	361	3.2	402	4.3	
314	355	1.8	384	7.1	
	336	1.4	365	10.1	
	327	-1.1	355	3.9	
	312	1.4	336	8.4	
	305	0.3	315	5.0	
			306	-0.8	
293	297	-3.0	287	2.5	Librations and translations of $\text{WO}_4^{2-}$
248	284	-2.4	266	-0.2	
201	269	3.2	244	8.0	
163	252	-1.2	219	6.1	
134	216	2.7	193	3.4	
120	202	2.9	177	-1.4	
93	189	4.4	142	-0.4	
	168	4.1	137	-3.0	
	143	1.0	123	3.1	
	139	0.6	118	1.2	
	119	0.8	109	1.8	
	116	-0.5	103	-0.5	
	107	-0.1	89	2.0	
	104	0.0	86	-0.1	
	95	-0.7			

octahedra. As a result, a significant distortion of the tetrahedral units would require much higher pressure than in case of  $\text{Sc}_2(\text{MoO}_4)_3$ . We suppose that as a result of the 2.8 GPa transition in  $\text{Al}_2(\text{WO}_4)_3$ , some rotations/tilts of the tungstate tetrahedra occur. The weak changes in energies and intensities of internal modes indicate that these rotations are accompanied by weak changes in the W–O bond lengths and O–W–O bond angles. Because the  $\text{WO}_4^{2-}$  tetrahedra and  $\text{AlO}_6$  octahedra share oxygen atoms, the rotations of the tungstate ions must also lead to some changes in the coordination sphere of  $\text{Al}^{3+}$  ions. We would also like to emphasize that this transition is most likely not the same as reported by Liu et al. at 2.8–3.2 GPa since these authors performed the study at 400°C and their X-ray results suggest transition into a tetragonal phase, whereas our studies

were performed at ambient temperature and the observed appearance of new modes is not consistent with symmetry increase. We would also like to point out that the compressibility and resistivity studies failed to discover this transition [15]. This result confirms that  $\text{Al}_2(\text{WO}_4)_3$  experiences weak changes at this transition. In such cases vibrational spectroscopy is more suitable tool for studying phase transitions since this technique is known to be very sensitive for slight changes in local symmetry and chemical bond strengths.

For completeness sake we show in Fig. 1 the Raman spectra for  $\text{Al}_2(\text{WO}_4)_3$  recorded during decompression run. It can be clearly seen that the lower trace in Fig. 1(b) and (d) is the same as the lower trace in Fig. 1(a) and (c). Therefore, this result indicates that both pressure-induced phase transformations in

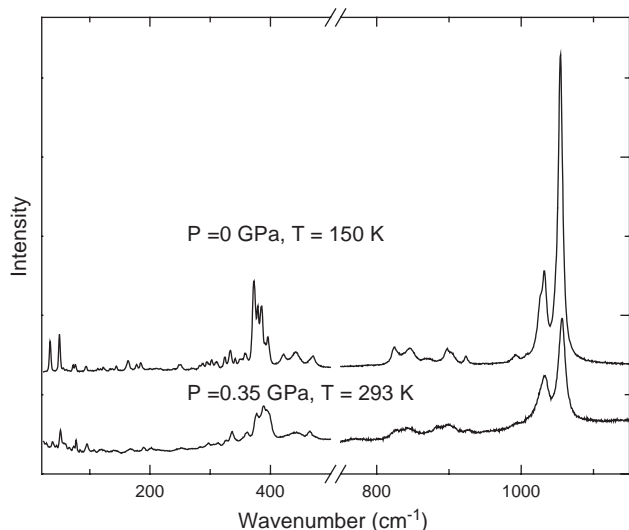


Fig. 3. Raman spectrum recorded at room temperature and 0.35 GPa pressure (lower trace) and ambient pressure and 150 K temperature (upper trace).

$\text{Al}_2(\text{WO}_4)_3$  are reversible, albeit we have observed some small hysteresis in the pressure transition values.

#### 4. Conclusions

High-pressure Raman study confirmed the onset of a reversible pressure-induced phase transformation in  $\text{Al}_2(\text{WO}_4)_3$  at around  $0.28 \pm \text{GPa}$ , discovered recently with the use of resistivity and compressibility measurements. The present results give strong indication that this transition occurs from the orthorhombic ( $D_{2h}^{14}$ ) to monoclinic ( $C_{2h}^5$ ) phase. The same mechanism was also observed previously for isomorphous  $\text{Sc}_2(\text{MoO}_4)_3$ , proving that the orthorhombic structure of  $A_2(\text{BO}_4)_3$  molybdates and tungstates is not stable and can be easily transformed into more dense phase. The present results show also the onset of another phase transformation at about 2.8 GPa. We argue that this transition leads to only slight modification of the crystal structure due to rotations/tilts of nearly rigid  $\text{WO}_4^{2-}$  tetrahedra. The significant increase in the bandwidth of many bands suggests the presence of some disordering in the phase stable above 2.8 GPa.

#### Acknowledgments

W.P. and A.G.S.F. acknowledge financial support from the Brazilian agencies CNPq and CAPES (PRODOC Grant No. 22001018), respectively. M.M. acknowledges UFC for supporting the visit to UFC. The Brazilian authors acknowledge partial support from Brazilian agencies (FUNCAP, CNPq and FINEP).

#### References

- [1] A.W. Sleight, L.H. Brixner, *J. Solid State Chem.* 7 (1973) 172.
- [2] A.K. Tyagi, S.N. Achary, M.D. Mathews, *J. Alloys Compd.* 339 (2002) 207.
- [3] J.S.O. Evans, T.A. Mary, *Int. J. Inorg. Mater.* 2 (2000) 143.
- [4] J.S.O. Evans, T.A. Mary, A.W. Sleight, *J. Solid State Chem.* 133 (1997) 580.
- [5] J.S.O. Evans, T.A. Mary, A.W. Sleight, *Physica B* 241–243 (1998) 311.
- [6] J.S.O. Evans, T.A. Mary, A.W. Sleight, *J. Solid State Chem.* 137 (1998) 148.
- [7] N. Imanaka, S. Tamura, G. Adachi, Y. Kowada, *Solid State Ionics* 130 (2000) 179.
- [8] N. Imanaka, S. Tamura, Y. Kobayashi, Y. Okazaki, M. Hiraiwa, T. Ueda, G. Adachi, *J. Alloys Compd.* 303–304 (2000) 303.
- [9] Y. Okazaki, T. Ueda, S. Tamura, N. Imanaka, G. Adachi, *Solid State Ionics* 136–137 (2000) 437.
- [10] R.A. Secco, H. Liu, N. Imanaka, G. Adachi, M.D. Rutter, *J. Phys. Chem. Solids* 63 (2002) 425.
- [11] R.A. Secco, H. Liu, N. Imanaka, G. Adachi, *J. Mater. Sci. Lett.* 20 (2001) 1339.
- [12] W. Paraguassu, M. Maczka, A.G. Souza Filho, P.T.C. Freire, J. Mendes Filho, F.E.A. Melo, L. Macalik, L. Gerward, J. Staun Olsen, A. Waskowska, J. Hanuza, *Phys. Rev. B*, in press.
- [13] H. Liu, R.A. Secco, N. Imanaka, M.D. Rutter, G. Adachi, T. Uchida, *J. Phys. Chem. Solids* 64 (2003) 287.
- [14] J. Hanuza, M. Maczka, K. Hermanowicz, M. Andruszkiewicz, A. Pietraszko, W. Streck, P. Deren, *J. Solid State Chem.* 105 (1993) 49.
- [15] G.D. Mukherjee, S.N. Achary, A.K. Tyagi, S.N. Vaidya, *J. Phys. Chem. Solids* 64 (2003) 611.
- [16] M. Maczka, J. Hanuza, E.T.G. Lutz, J.H. van der Maas, *J. Solid State Chem.* 145 (1999) 751.
- [17] T.R. Ravindran, A.K. Arora, T.A. Mary, *J. Phys.: Condens. Matter* 13 (2001) 11573.
- [18] T.R. Ravindran, A.K. Arora, T.A. Mary, *Phys. Rev. Lett.* 84 (2000) 3879.